Chinese Chemical Letters 32 (2021) 3185–3188

Contents lists available at ScienceDirect

Chinese Chemical Letters

journal homepage: www.elsevier.com/locate/cclet

Communication

Bird nest-like zinc oxide nanostructures for sensitive electrochemical glucose biosensor

Feng Shi[a,1], Jinming Xu[a,1], Zhongfang Hu[a,1], Chuanli Ren[d], Yadong Xue[c,*], Yongcai Zhang[a], Juan Li[a,*], Chengyin Wang[a], Zhanjun Yang[a,b,**]

[a] School of Chemistry and Chemical Engineering, Yangzhou University, Yangzhou 225002, China
[b] Guangling College, Yangzhou University, Yangzhou 225002, Zhenjiang Precise Intelligent Technology Co. Ltd., Zhenjiang 212016, China
[c] Central Laboratory, Affiliated Jinhua Hospital, Zhejiang University School of Medicine, Jinhua 321000, China
[d] Department of Laboratory Medicine and Clinical Medical College of Yangzhou University, Yangzhou 225001, China

ARTICLE INFO

Article history:
Received 13 November 2020
Received in revised form 20 December 2020
Accepted 3 March 2021
Available online 9 March 2021

Keywords:
Bird nest-like zinc oxide
Nanostructure
Glucose oxidase
Electrochemical
Biosensor

ABSTRACT

In this research, a novel bird nest-like zinc oxide (BN-ZnO) nanostructures were prepared by a simple solvothermal method. A sensitive electrochemical glucose biosensor was for the first time developed based on the immobilization of glucose oxidase (GOx) on nanostructured BN-ZnO modified electrode. The BN-ZnO nanostructure and the resultant biosensor were characterized by scanning electron microscope, X-ray diffraction spectroscopy, Fourier transform infrared spectroscopy, and electrochemical impedance spectroscopy. BN-ZnO nanostructures have large specific surface area and can load large amounts of GOx molecules. Meanwhile, BN-ZnO provides an excellent microenvironment to retain the native bioactivity of enzymes and to promote direct electron transfer between GOx and electrode surface. The proposed biosensor shows a wide linear range of 0.005–1.6 mmol/L, high sensitivity of 15.6 mA L mol^{-1} cm^{-2} with a low detection limit of 0.004 mmol/L. The resulting biosensor also shows excellent selectivity, acceptable stability and reproducibility, and can be successfully applied in the detection of glucose in human serum samples at −0.37 V.

Diabetes mellitus disrupts the regulation of the body's blood glucose levels. Poorly regulated blood glucose levels can lead to serious diseases such as kidney failure, heart disease, and blindness [1]. The measurements of blood glucose show an important significance in the treatment and monitoring of diabetes mellitus [2]. Tremendous amount of electrochemical biosensors have been widely developed to measure glucose due to high sensitivity, fast analysis speed, high selectivity, simple instrument operation as well as low cost [3–11]. Among these biosensors, the third-generation enzyme biosensors based on direct electron transfer have showed great potentials [12,13]. However, it hard to achieve the direct electron transfer of glucose oxidase (GOx) because the active redox center (flavin adenine dinucleotide, FAD) of GOx is deeply embedded within a protective protein shell. Modifications of electrode with nanomaterials have been proved to be an effective method to overcome the long distance between the redox-active cofactor and the electrode surface [13–16]. Many kinds of nanomaterials such as metal nanoparticles [17–19], carbon nanomaterials [12,20,21] and semiconductor nanostructures [22–24] have been extensively used to modify electrode surface to promote the direct electron transfer.

Zinc oxide (ZnO) is a typical semiconductor material and exhibits unique chemical properties [25]. ZnO materials have been applied to a wide variety of fields such as lithium batteries [26], solar cells [27], and photocatalysts [28]. In the past decades, nanostructured ZnO has gained great attention in biosensing fields due to good chemical stability, nontoxicity, high surface to volume ratio, biocompatibility, and easy fabrication [29,30]. Various shaped ZnO nanostructures, such as nanoparticles [31,32], nanorods [33,34] nanowires [35,36], flowers [37] and nanospheres [38] have been reported for biosensing using vapor deposition or wet chemical methods. It has been well demonstrated that enzyme biomolecules immobilized on ZnO nanostructures can enhance its catalytic ability, accelerate the direct electron transfer and retain the bioactivity [39]. Moreover, morphology and size of nanostructured ZnO materials also play a very important role in the

* Corresponding authors.
** Corresponding author at: School of Chemistry and Chemical Engineering, Yangzhou University, Yangzhou 225002, China.
E-mail addresses: xueyadong@zju.edu.cn (Y. Xue), lijuan@yzu.edu.cn (J. Li), zjyang@yzu.edu.cn (Z. Yang).
[1] These authors contributed equally to this work.

https://doi.org/10.1016/j.cclet.2021.03.012

properties of the glucose biosensors [24,30]. Thus it is very necessary to explore synthesis of suitable shaped and sized ZnO materials for the enzyme biosensors. To the best of our knowledge, there are few bird nest-like ZnO (BN-ZnO) nanostructures for biosensing applications.

In this research, novel BN-ZnO nanostructures were synthesized by a simple solvothermal route from $ZnCl_2$, CON_2H_4, ethanol and HCl. The morphology and composite of BN-ZnO nanostructure were confirmed using scanning electron microscope (SEM) and X-ray diffraction spectroscopy (XRD). Then BN-ZnO nanostructures were for the first time exploited to modify electrode for the immobilization of enzymes. A sensitive electrochemical biosensor was proposed to measure glucose based on direct chemistry of GOx on modified electrode. BN-ZnO nanostructures have larger surface area and provided a biocompatible microenvironment to facilitate the direct electron transfer from electrode surface to the immobilized enzyme. The proposed biosensor demonstrated high sensitivity, excellent selectivity and acceptable producibility and stability. This work provided a promising electrode material for the fabrication of excellent biosensors.

The morphology of the as-synthesized BN-ZnO nanostructure was investigated using scanning electron microscope. Fig. 1A shows the SEM image of BN-ZnO, and Fig. 1B shows its magnification of the nanostructure. It can be seen that the BN-ZnO displays bird nest-shaped structure and uniform appearance with a particle size of about 10 μm, which consists of nano-sized thin sheets. This special structure results to big large specific surface area. A typical XRD pattern of the as-synthesized BN-ZnO was shown in Fig. 1C. All of the diffraction peaks can be exactly indexed to the single hexagonal phase ZnO (JCPDS No. 076-0704). After the immobilization of GOx on BN-ZnO modified electrode, the SEM of GOx/BN-ZnO (Fig. 1D) shows the different morphology in comparison with singe BN-ZnO. In other words, these changes in the morphology of BN-ZnO indicate the successful modification of GOx on the surface BN-ZnO.

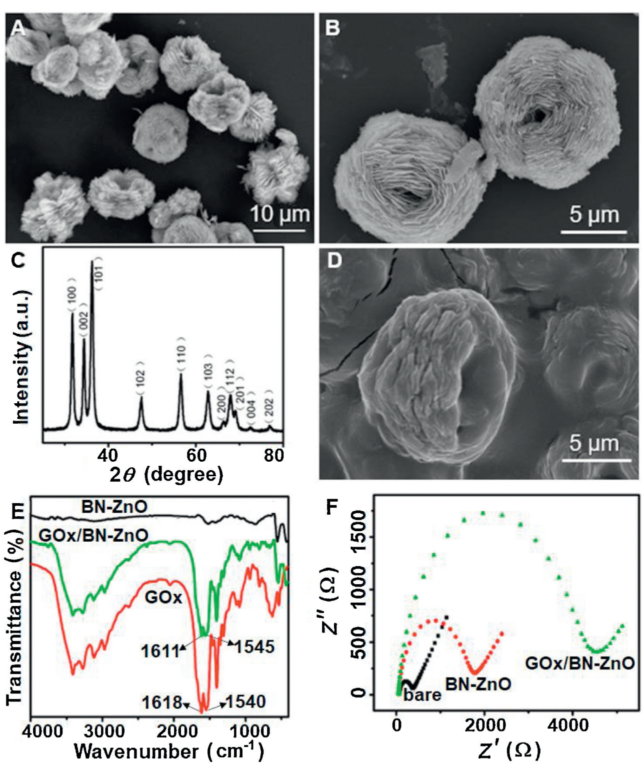

Fig. 1. SEM image of BN-ZnO and its magnification (A, B), XRD pattern of the as-synthesized BN-ZnO (C), SEM of GOx/BN-ZnO (D), FT-IR spectrum of BN-ZnO, GOx, GOx/BN-ZnO (E), EIS of bare, BN-ZnO and GOx/BN-ZnO modified electrodes (F).

FT-IR spectrum was used to characterize the structure of the GOx molecules loaded on BN-ZnO (Fig. 1E). No obvious absorption peaks were observed from the FT-IR spectrum of BN-ZnO. The FT-IR spectrum of native GOx exhibits two characteristic peaks at 1611 and 1545 cm^{-1}, which are ascribed to amide I and II bands of enzyme. FT-IR spectrum of the GOx/BN-ZnO also shows two characteristic absorption peaks of amide I and amide II bands, indicating that GOx molecules were successfully immobilized in the BN-ZnO nanostructure and maintain its native structure and bioactivity. Electrochemical impedance spectroscopy was employed to study the surface property and process for the modified electrodes. The impedance spectrum is named as Nyquist plot which comprises a semicircle part and a liner part. The semicircle at the high frequency corresponds to the electron-transfer in the limiting process, whose diameter presents the electron transfer resistance (R_{ct}). And the straight line at the low frequency corresponds to the dispersion process. Fig. 1F shows the electrochemical impedance spectra (EIS) of different modified electrodes in the frequency range of 0.05 Hz to 10 KHz. For the bare GCE, the R_{ct} was about 298 Ω. The R_{ct} of the BN-ZnO/GCE (1669 Ω) was larger than that of the bare GCE, demonstrating that a layer of BN-ZnO film was formed on the surface of GCE. After GOx was immobilized on the surface of BN-ZnO nanostructure, its R_{ct} value further increased to 4171 Ω, which indicated that GOx molecules were steadily absorbed into the surface of BN-ZnO modified electrode.

Fig. 2 shows the cyclic voltammograms (CVs) of different modified GCEs in 0.1 mol/L N_2-saturated PBS at a scan rate of 100 mV/s. No peaks were observed from the CV curves of the Nafion/GCE (curve a) and BN-ZnO/Nafion/GCE (curve b). However, the GOx/Nafion/GCE shows a pair of weak and well-defined redox peaks (curve c). Compared with GOx/Nafion/GCE, the GOx/BN-ZnO/Nafion/GCE displays a pair of intensive and better-defined redox peaks (curve d) at -0.342 and -0.387 V, indicating that BN-ZnO effectively facilitate direct electron transfer of GOx and electrode surface. The reduction peak current of the GOx/BN-ZnO/Nafion/GCE is 4 times larger than that of GOx/Nafion/GCE, which may result from the special nanostructure and larger specific surface of BN-ZnO nanostructure [39].

The influence of the pH value on the electrochemical behavior of the GOx/ BN-ZnO/Nafion/GCE was examined in Fig. S1A (Supporting information). Both the cathodic and anodic peak potentials shift negatively with the increase of the solution pH values. The formal potential demonstrated a linear relationship with a slope of −48.9 mV/pH and a correlation coefficient of 0.9852 (inset I of Fig. S1A), suggesting that the enzymatic reaction of GOx/BN-ZnO/Nafion/GCE is same-electron coupled same-proton transfer process. The redox peaks current reached its maximum value at pH 7.0, suggesting the optimal solution pH for the immobilization of GOx (inset II of Fig. S1A). The decreases in

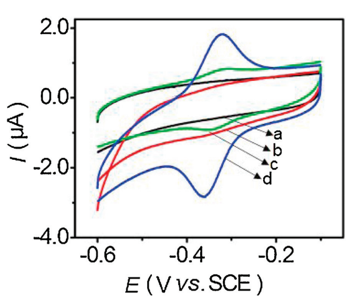

Fig. 2. CVs of bare GCE (a), BN-ZnO/GCE (b), GOx/GCE (c) and BN-ZnO/GOx/GCE (d) in 0.1 mol/L pH 7.0 N_2-saturated PBS at a scan rate of 100 mV/s.

current response at higher pH value or lower pH value are possible due to decreased bioactivity of the loaded enzyme molecules [40].

The CVs of GOx/BN-ZnO/Nafion/GCE at different scan rates were shown in Fig. S1B (Supporting information). It could be observed that the anodic current (I_{pa}) and cathodic peak current (I_{pc}) linearly enhanced with the increasing scan rate from 10 to 300 mV/s (inset I of Fig. S1B). Moreover, the ratio of I_{pa} and I_{pc} is close to 1.0, suggesting that electrochemical reactions of GOx on BN-ZnO modified electrode was quasi-reversible surface-controlled process [41]. The logarithm plot of cathodic peak current demonstrated a good linear relationship versus logarithm of the scan rate with a slope of 0.9755 (inset II of Fig. S1B). The slope is very close to the theoretical slope for thin layer electrochemical behavior.

Fig. 3 shows the CVs of the BN-ZnO/Nafion/GCE and GOx/BN-ZnO/Nafion/GCE in nitrogen- and air-saturated pH 7.0 PBS in the absence and presence of glucose. No obvious redox peak could be observed from CVs of BN-ZnO/Nafion/GCE in air-saturated PBS, but a reduction peak current enhanced obviously at more negative potential (curve b of Fig. 3A). When glucose was added into this air-saturated solution, the reduction peak current of the BN-ZnO/Nafion/GCE shows no obvious change (curves c and d of Fig. 3A). As a contrast, GOx/BN-ZnO/Nafion/GCE shows an obvious redox peaks, and its reduction peak current obviously enhanced in air-saturated solution (curve f of Fig. 3B). As illustrated in Eqs. 1 and 2, this phenomenon indicating a typical electrocatalytic process toward dissolved oxygen occurred at GOx/BN-ZnO/Nafion/GCE instead of BN-ZnO/Nafion/GCE. While glucose was added into this system, gradual decreases in reduction peak current at the GOx/BN-ZnO/Nafion/GCE was observed clearly (curves g and h of Fig. 3B). This was because that the enzyme-catalyzed reaction at GOx/BN-ZnO/Nafion/GCE inhibited the electrocatalytic reaction, which leaded to the decrease of GOx (FAD) according to Eq. 3. Based on the responses of the GOx/BN-ZnO/Nafion/GCE to glucose, an electrochemical enzyme biosensor was constructed for quantitative detection of glucose.

$$\mathrm{GOx(FAD)} + 2e^- + 2H^+ \leftrightarrow \mathrm{GOD(FADH_2)} \quad (1)$$

$$\mathrm{Glucose} + \mathrm{GOx(FAD)} \rightarrow \mathrm{GOx(FADH_2)} + \mathrm{Gluconolactone} \quad (2)$$

$$\mathrm{GOx(FADH_2)} + O_2 \rightarrow \mathrm{GOD(FAD)} + H_2O_2 \quad (3)$$

Fig. 4A shows the amperometric response of the GOx/Nafion/GCE and GOx/BN-ZnO/Nafion/GCE in pH 7.0 air-saturated PBS containing different concentrations of glucose at –0.37 V applied potential. The current responses of GOx/BN-ZnO/Nafion/GCE increased linearly with the increase of glucose concentration ranging from 0.005 mmol/L to 1.6 mmol/L with a high sensitivity of 15.6 mA L mol^{-1} cm^{-2} (Fig. 4A). The detection limit is calculated to be 4.0 μmol/L at a signal-to-noise of 3. As a contrast, the

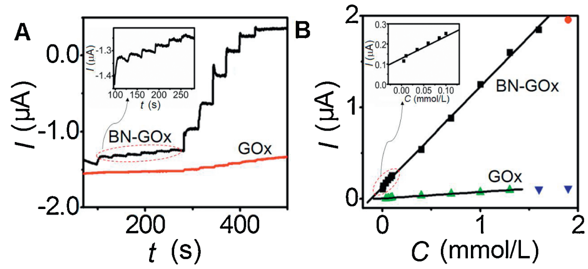

Fig. 4. Amperometric response of Nafion/GOx/ BN-ZnO/GCE and Nafion/GOx/GCE to successive additions of glucose in a stirred 0.1 mol/L pH 7.0 PBS at an applied potential of –0.37 V, inset: magnified amperometric response *versus* time (A) and calibration curves for glucose concentration, inset: magnified calibration curve (B).

GOx/Nafion/GCE shows a linear range of 0.035–1.3 mmol/L with a detection limit of 30 μmol/L (Fig. 4B). Compared with the GOx/Nafion/GCE, the GOx/BN-ZnO/Nafion/GCE demonstrated much higher sensitivity and wider linear range. Obviously, BN-ZnO nanostructure greatly promoted the direct electron transfer between GOx and electrode surface, thus producing high sensitivity. The performance of present glucose biosensor was compared with other glucose biosensors reported in recent literatures and shown in Table S1 (Supporting information). In comparison with other types of enzyme electrodes, the proposed GOx/BN-ZnO/Nafion/GCE shows better excellent performance.

The reproducibility of the proposed biosensor was investigated by detecting 0.1 mmol/L glucose for 5 times at same enzyme electrode, the relative standard deviation (RSD) is 3.5%, indicating a good repeatability. After 20 successive measurements, the current response still retained 92% of the initial value, suggesting acceptable operational stability. The reproducibility of the enzyme electrode was also examined by measuring 0.1 mmol/L glucose at 5 different enzyme electrodes, and the RSD was 6.5%, indicating good fabrication reproducibility. The enzyme electrode was stored at 4 °C when not in use. It can be retained 93% of its initial current response after storage for three weeks, demonstrating the acceptable long-term life time of the BN-ZnO-based glucose biosensor.

Fig. 5 shows the interferences in quantitative detection of glucose in the presence of 0.1 mmol/L uric acid (AA), 0.1 mmol/L ascorbic acid (AP), and 0.1 mmol/L acetamidophenol (UA) at an applied potential of −0.37 V. Upon the addition of 0.1 mmol/L glucose to pH 7.0 electrolyte solution, a clear current response could be observed. When the AA, AP and UA were successively injected into the solution, there were no obvious changes in the amperometric response. After addition of 0.1 mmol/L glucose to the system again, the current response is almost close to the value obtained in absence of the interferents, suggesting the excellent selectivity of the constructed electrochemical glucose biosensor.

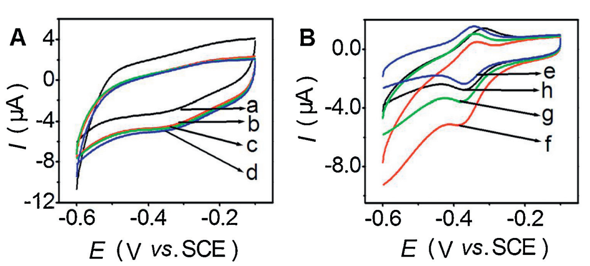

Fig. 3. CVs of the BN-ZnO/Nafion/GCE (A) and GOx/ BN-ZnO/Nafion/GCE (B) in 0.1 mol/L pH 7.0 N_2-saturated PBS (a and e), air-saturated PBS (b and f), air-saturated PBS including 0.5 mmol/L glucose (c and g) and 1.0 mmol/L glucose (d and h) at a scan rate of 100 mV/ s.

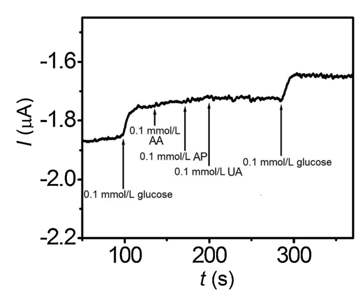

Fig. 5. Amperometric response of the GOx/BN-ZnO/Nafion/GCE to 0.1 mmol/L glucose, 0.1 mmol/L AA, 0.1 mmol/L AP, and 0.1 mmol/L UA in 0.1 mol/L pH 7.0 PBS at –0.37 V applied potential.

To evaluate the potential ability of the BN-ZnO-based biosensor, the human serum samples were measured. The practical samples were received from Northern Jiangsu People's Hospital without any sample pretreatment except a dilution step and their glucose concentrations were determined using enzyme catalytic spectrophotometry. The results of human serum samples measured by two methods were showed in Table S2 (Supporting information). The relative errors between two methods are no more than 8.7%, showing good accuracy of the present biosensor in the detection of the real samples.

In this work, bird nest-like ZnO nanostructures were prepared by a simple solvothermal method. The morphology and properties of BN-ZnO nanostructures were characterized using several methods. Based on the direct electron transfer of GOx immobilized on BN-ZnO nanostructure modified electrode, a novel electrochemical glucose biosensor was developed for the first time. BN-ZnO nanostructure provides a favorable microenvironment for GOx to remain its bioactivity and enhances the electron transfer between enzyme and the electrode surface. Thus the biosensor modified with BN-ZnO nanostructure shows a better detection range than the biosensor without BN-ZnO nanostructure. The glucose biosensor also exhibits excellent selectivity, good reproducibility, and acceptable stability. The BN-ZnO nanostructure provide a promising platform for fabricating excellent electrochemical biosensors.

Declaration of competing interest

The authors declare that they have no known competing financial interests or personal relationships that could have appeared to influence the work reported in this paper.

Acknowledgments

The authors acknowledge the financial support from the National Natural Science Foundation of China (Nos. 21575125, 21475116), the Natural Science Foundation of Jiangsu Province (No. BK20191434), 333 Project and Qinglan Project of Jiangsu Province, and high-end talent support program of Yangzhou University for Zhanjun Yang, and Juan Li, Priority Academic Program Development of Jiangsu Higher Education Institution (PAPD), Six Talent Peaks Project of Jiangsu Province for Zhanjun Yang and Juan Li, Project for Science and Technology of Yangzhou (No. YZ2020068), the Project for Science and Technology of Zhenjiang (No. GY2020028), Zhejiang Provincial Natural Science Foundation of China (No. LY20B050008), Zhejiang Provincial Project of Medical and Health Technology (No. 2021RC139), and Key Project of Social Development of Jinhua (No. 2020-3-033).

Appendix A. Supplementary data

Supplementary material related to this article can be found, in the online version, at doi:https://doi.org/10.1016/j.cclet.2021.03.012.

References

[1] C. Pickup, Z.L. Zhi, F. Khan, T. Saxl, D.J.S. Birch, Diabetes-Metab. Res. & Rew. 24 (2008) 604–609.
[2] C. Pickup, F. Hussain, N.D. Evans, N. Sachedina, Biosens. Bioelectron. 20 (2005) 1897–1902.
[3] J. Li, Y. Liu, X. Tang, et al., Microchim. Acta 187 (2020) 80.
[4] P. Yao, S.H. Yu, H.F. Shen, et al., New J. Chem. 43 (2019) 16748–16752.
[5] C.S. Zhou, Y.L. Shi, X.D. Ding, et al., Anal. Chem. 85 (2013) 1171–1176.
[6] J. Li, Y. Tang, J. Yang, et al., Sens. Actuators B: Chem. 190 (2014) 549–554.
[7] Z.F. Hu, R. Xu, S.H. Yu, J. Li, Z.J. Yang, Analyst 145 (2020) 7864–7869.
[8] Y.L. Wu, Q.W. Li, X.L. Zhang, X. Chen, X.M. Wang, Chin. Chem. Lett. 24 (2013) 1087–1090.
[9] S. Tang, X.Z. Wang, J.P. Lei, et al., Biosens. Bioelectron. 26 (2010) 432–436.
[10] J. Li, M.M. Lu, Z.N. Tan, et al., Microchim. Acta 183 (2016) 1705–1712.
[11] X. Xu, S.J. Jiang, Z. Hu, S.Q. Liu, ACS Nano 4 (2010) 4292–4298.
[12] X.H. Kang, J. Wang, H. Wu, et al., Biosens. Bioelectron. 25 (2009) 901–907.
[13] J. Wang, Chem. Rev. 108 (2008) 814–825.
[14] C.S. Shan, H.F. Yang, J.F. Song, et al., Anal. Chem. 81 (2009) 2378–2382.
[15] B. Liang, L. Fang, G. Yang, et al., Biosens. Bioelectron. 43 (2013) 131–136.
[16] J.T. Holland, C. Lau, S. Brozik, P. Atanassov, S. Banta, J. Am. Chem. Soc. 133 (2011) 19262–19265.
[17] S.Q. Liu, H.X. Ju, Biosens. Bioelectron. 19 (2003) 177–183.
[18] Y.H. Ye, H.Q. Xie, X.B. Shao, et al., J. Nanosci. Nanotechnol. 16 (2016) 2270–2276.
[19] Y.H. Song, J.Y. Chen, H.Y. Liu, et al., Anal. Chem. Acta. 891 (2015) 144–150.
[20] B.R. Azamian, J.J. Davis, K.S. Coleman, C.B. Bagshaw, M.L.H. Green, J. Am. Chem. Soc. 124 (2002) 12664–12665.
[21] S.Y. Deng, G.Q. Jian, J.P. Lei, Z. Hu, H.X. Ju, Biosens. Bioelectron. 25 (2009) 373–377.
[22] Y.L. Zhou, S.D. Uzun, N.J. Watkins, et al., ACS Appl. Mater. Interfaces 11 (2019) 1821–1828.
[23] S.J. Bao, C. Li, J.F. Zang, et al., Adv. Funct. Mater. 18 (2018) 591–599.
[24] Z.J. Yang, Y.Y. Ren, Y.C. Zhang, et al., Biosens. Bioelectron. 26 (2011) 4337–4341.
[25] N.K. Park, Y.J. Lee, G.B. Hana, et al., Colloids and Surfaces A: Physicochem. Eng. Aspects 313 (2008) 66–71.
[26] L.R. Hou, L. Lian, L.H. Zhang, et al., Adv. Funct. Mater. 25 (2015) 238–246.
[27] Y.Q. Wang, X. Cui, Y. Zhang, X.R. Gao, Y.M. Sun, J. Mater. Sci. Technol. 29 (2013) 123–127.
[28] X.T. Chang, Z.L. Li, X.X. Zhai, et al., Mater. Des. 98 (2016) 324–332.
[29] V. Arabali, M. Ebrahimi, H. Karimi-Maleh, Chin. Chem. Lett. 27 (2016) 779–782.
[30] H.J. Zhang, N. Patel, J. Xiong, S. Ding, RSC Adv. 5 (2015) 85720–85729.
[31] Z. Shu, Y. Zhang, Q. Yang, H.M. Yang, Nanoscale Res. Lett. 12 (2017) 135.
[32] J. Safaei-Ghomi, M.A. Ghasemzadeh, Chin. Chem. Lett. 23 (2012) 1225–1229.
[33] H. Sajjadi-Ghotbabadi, S. Javanshir, Chin. Chem. Lett. 28 (2017) 274–279.
[34] H. Ma, Semiconductors 53 (2019) 1811–1816.
[35] W.J. Zheng, W.C. Tzou, J.R. Shen, C.F. Yang, C.C. Chen, Sensor. Mater. 31 (2019) 447–455.
[36] S. Park, S. Kim, H. Ko, C. Lee, J. Nanosci. Nanotechnol. 15 (2015) 5301–5305.
[37] H. Zhang, D. Yang, Y.J. Ji, et al., J. Phys. Chem. B 108 (2004) 3955–3958.
[38] M. Sasmal, T.K. Maiti, T.K. Bhattacharyya, IEEE Trans. Nanobiosci. 14 (2015) 129–137.
[39] Z.H. Dai, G.J. Shao, J.M. Hong, J.C. Bao, Biosens. Bioelectron. 24 (2009) 1286–1291.
[40] D. Wen, Y. Liu, G.C. Yang, S.J. Dong, Electrochim. Acta 52 (2007) 5312–5317.
[41] C.G. Tian, Q. Zhang, B.J. Jiang, G.H. Tian, H.G. Fu, J. Alloys. Compd. 509 (2011) 6935–6941.